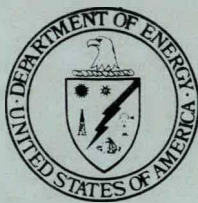


# RADIATION LABORATORY UNIVERSITY of NOTRE DAME



Quarterly Report

Received by OSTI

MAY 22 1989

January 1 - March 31, 1989

DO NOT MICROFILM  
THIS PAGE

DISTRIBUTION OF THIS DOCUMENT IS UNLIMITED

## **DISCLAIMER**

**This report was prepared as an account of work sponsored by an agency of the United States Government. Neither the United States Government nor any agency thereof, nor any of their employees, makes any warranty, express or implied, or assumes any legal liability or responsibility for the accuracy, completeness, or usefulness of any information, apparatus, product, or process disclosed, or represents that its use would not infringe privately owned rights. Reference herein to any specific commercial product, process, or service by trade name, trademark, manufacturer, or otherwise does not necessarily constitute or imply its endorsement, recommendation, or favoring by the United States Government or any agency thereof. The views and opinions of authors expressed herein do not necessarily state or reflect those of the United States Government or any agency thereof.**

---

## **DISCLAIMER**

**Portions of this document may be illegible in electronic image products. Images are produced from the best available original document.**

**RADIATION LABORATORY**  
**UNIVERSITY OF NOTRE DAME**

**QUARTERLY REPORT**

**January 1 - March 31, 1989**

**DISCLAIMER**

This report was prepared as an account of work sponsored by an agency of the United States Government. Neither the United States Government nor any agency thereof, nor any of their employees, makes any warranty, express or implied, or assumes any legal liability or responsibility for the accuracy, completeness, or usefulness of any information, apparatus, product, or process disclosed, or represents that its use would not infringe privately owned rights. Reference herein to any specific commercial product, process, or service by trade name, trademark, manufacturer, or otherwise does not necessarily constitute or imply its endorsement, recommendation, or favoring by the United States Government or any agency thereof. The views and opinions of authors expressed herein do not necessarily state or reflect those of the United States Government or any agency thereof.

**ISSUED**

**April 28, 1989**

**MAS**

**DISTRIBUTION OF THIS DOCUMENT IS UNLIMITED**

*DP*

The Notre Dame Radiation Laboratory is a facility of the Department of Energy operated for DOE by the University of Notre Dame under contract No. DE-AC02-76ER00038. The majority of the programs within the Laboratory are supported by the Office of Basic Energy Sciences of DOE and, unless otherwise noted in the following, support can be attributed to the Office of Basic Energy Sciences. Certain additional programs, so indicated, are supported by the Office of Standard Reference Data of the National Bureau of Standards.

\* \* \* \* \*

Mr. V. Rassolov, a student at the Moscow Institute for Physics and Technology who is presently associated with the Notre Dame Institute for International Peace Studies, began a research project under the supervision of Prof. R. H. Schuler on 1/4/89.

Dr. E. Baumgartner of the Comision Nacional de Energia Atomica, Buenos Aires, Argentina, joined the Laboratory on 1/7/89, on a fellowship supported jointly by the American Chemical Society and the Asociacion Quimica Argentina. Dr. Baumgartner will collaborate with Dr. G. Ferraudi on studies in inorganic photochemistry.

Mr. S. Pommeret of the Ecole Nationale Superieure de Techniques Avancees, Paliseau, France, joined us on 2/12/89 as a Research Associate. Mr. Pommeret will be conducting theoretical studies of the hydrated electron.

Mr. D. Markovic of the University of Nis, Yugoslavia, and a graduate student under the supervision of Dr. L.K. Patterson, returned to his home institution on 2/4/89. He will rejoin the Laboratory later this year to continue his studies.

Dr. M. Bohorquez completed her appointment as Research Associate and left the Laboratory to accept a position at Bowling Green State University on 3/31/89.

\* \* \* \* \*

Visitors during the past quarter included the following:

Dr. E.W. Boyer of Miles Laboratories, Elkhart, visited the Laboratory on 1/19/88 to conduct some radiolysis experiments.

Prof. D. Armstrong of the University of Calgary spent the period 1/25-2/1/89 conducting radiolysis experiments on the LINAC.

Dr. A. Hitachi of Waseda University, Japan, visited us for the period 2/17-3/25/89 to assemble apparatus for an experiment to be conducted later this year.

Publications

P. Natarajan

Photochemistry of Macromolecular Dyes in Aqueous Solutions.

J. Macromol. Sci.-Chem. A25, 1285 (1988) [NDRL 3036]

P.V. Kamat and W.E. Ford

Photochemistry on Surfaces: 2. Intermolecular Electron Transfer on Colloidal Alumina-Coated Silica Particles.

J. Phys. Chem. 93, 1405 (1989) [NDRL 3054]

P.V. Kamat

Photoelectrochemistry in Particulate Systems. 9. Photosensitized Reduction in a Colloidal  $TiO_2$  System Using Anthracene-9-carboxylic Acid as the Sensitizer.

J. Phys. Chem. 93, 859 (1989) [NDRL 3068]

M. Ye and R.H. Schuler

Second-Order Combination Reactions of Phenoxy Radical.

J. Phys. Chem. 93, 1898 (1989) [NDRL 3081]

B. Kraut and G. Ferraudi

Photochemical Reactivity in Molybdenum Clusters: Competition between Photo-substitution and Phosphorescence in  $Mo_6Cl_{14}^{2-}$ .

Inorganica Chimica Acta 156, 7 (1989) [NDRL 3096]

P.A. Politowicz, L.B.S. Leung and J.J. Kozak

Influence of Swelling on Reaction Efficiency in Intercalated Clay Minerals.

2. Pillared Clays.

J. Phys. Chem. 93, 923 (1989) [NDRL 3097]

K.R. Gopidas and P.V. Kamat

Photoelectrochemistry in Particulate Systems. 11. Reduction of Phenosafranin Dye in Colloidal  $TiO_2$  and  $CdS$  Suspensions.

Langmuir 5, 22 (1989) [NDRL 3100]

N.J.B. Green

On the Simulation of Diffusion Processes Close to Boundaries.

Molecular Physics 65, 1399 (1988) [NDRL 3108]

G. Mehta, S. Padma, S.R. Karra, K.R. Gopidas, D.R. Cyr, P.K. Das and M.V. George

Steady-State and Laser Flash Photolysis Studies of Norbornenobenzoquinones and Their Diels-Alder Adducts.

J. Org. Chem. 54, 1342 (1989) [NDRL 3114]

D.M. Chipman

Spin Densities of First-row Atoms Calculated from Polarization Wave Functions with Accurate Numerical Methods.

Phys. Rev. A, 39, 475 (1989) [NDRL 3115]

I. Carmichael

Isotropic Coupling Constants for the Atoms B-F from Correlated Calculations Based on Spin-Unrestricted Wave Functions.

J. Phys. Chem. 93, 190 (1989) [NDRL 3125]

A. Samanta and R.W. Fessenden

On the Triplet Lifetime and Triplet-Triplet Absorption Spectra of Naphthaldehydes.  
Chem. Phys. Lett. 153, 406 (1988) [NDRL 3129]

External Talks and Presentations

K. Madden, "A Time Resolved ESR Study of Nitrosoalkane Spin Trapping",  
University of Akron, January 31, 1989.

The following reports were issued during the period of the quarter:

1. (NDRL-3170) Phase Effects on the Differential Track Structure of Electrons in Water<sup>1</sup>

(J.A. LaVerne, N.J.B. Green, A. Mozumder and S.M. Pimblott)

The energy loss of electrons in water has been considered using a differential inelastic cross-section incorporating both exchange and relativistic effects. The cross-section was formulated in terms of the dipole oscillator strength distribution, which has been determined from experimental measurements in gaseous and liquid water and amorphous ice. The density normalized inelastic mean free path in the ice is only slightly greater than in the liquid, while both are considerably larger than in the gas especially at low electron energies. Even at the highest electron energies, the mean free path in the liquid is approximately 10% greater than in the gas. The differential energy loss spectrum of an incident electron can be obtained from the probability distribution function for energy loss events,  $Y$ , which is the normalized cumulative cross-section for inelastic processes. Contributions from secondary electrons are determined by a Monte Carlo method. It is found that the average energy loss per event by a 1 MeV electron in liquid water is about 60 eV and somewhat less for the gas phase.

---

(1) Submitted for presentation at 37th Annual Meeting of Radiation Research Society, Seattle, WA, March 19-23, 1989.

---

2. (NDRL-3171) Geminate Ion Recombination in Anisotropic Media. Effects of Initial Distribution and External Field.<sup>1</sup>

(S.M. Pimblott, A. Mozumder and N.J.B. Green)

Recently we presented [Chem. Phys. Lett. 142, 385 (1987)] a method for calculating the diffusion-controlled geminate escape probability of an ion pair in an anisotropic medium. The escape probability depends on both the length and the direction of the initial inter-ion vector, and is reducible to a function of two dimensionless variables describing the overall anisotropy of the medium. In this paper the treatment is extended to include an initial distribution of inter-ion distances and an external field. Inclusion of a field increases the number of independently variable parameters to five: two

to describe the anisotropy of the medium and three to describe the intensity and direction of the applied field. It is shown that the effects of including anisotropy are not negligible for the typical case of anthracene and that the slope-to-intercept ratio of the field-dependent escape probability for a spherically averaged distribution depends on the direction of the applied field.

---

(1) Submitted for publication in the *Journal of Chemical Physics*.

---

3. (NDRL-3172) Some Methods for Evaluating Glass Impellers and Closed Circulating Systems<sup>1</sup>

(I.B. Duncanson)

This paper presents some techniques for evaluating the performance of glass impellers and closed circulating systems. By using a video cassette recording system and a simple flow apparatus, it is possible to (1) qualitatively determine flow irregularities or impediments in a system; (2) estimate the time for a molecule to complete one cycle; and (3) estimate the rate of flow generated by an impeller unit. With this information, more efficient designs can be rationally effected for a given application.

---

(1) Submitted for presentation at the 34th Annual Symposium and Exposition of the American Scientific Glassblowers Society in Milwaukee, Wisconsin, June 28, 1989.

---

4. (NDRL-3173) Magnetic Field Effects in the Photochemistry of Coordination Compounds<sup>1</sup>

(G. Ferraudi and S. Ronco)

The effect of the magnetic field ( $0 \leq H \leq 9$  Tesla) on the rates of outer and inner sphere electron transfer reactions has been investigated as a function of the magnetic field intensity. In outer sphere cross reactions where Co(III) complexes were used as oxidants and Ru(II) or low spin-Co(II) complexes as reductants, the dependence of the rates on the magnetic field can be related to field-induced changes of the pre-exponential, i.e., electron coupling, and exponential, i.e., activation energy of magnetization, factors. Moreover, measurements of the activation energy of magnetization, in exper-

iments where the rates were measured as a function of the temperature at given field intensities, suggest that the transition state of these reactions is largely paramagnetic. The activation magnetic susceptibilities measured for Co(III)/Ru(II) reactions were in the order of  $10^2$  Joule/(Tesla) $^2$  M. Small field effects have been observed in inner sphere reactions between Co(III) and Fe(II) complexes. A mechanism for the magnetic field perturbation of the rate in electron transfer reactions and possible field-induced perturbations on the rates of excited state reactions will be discussed.

---

(1) Submitted for presentation at the 27th International Conference on Coordination Chemistry, Gold Coast, Australia, July 2-7, 1989.

---

5. (NDRL-3174) Stochastic Modelling of Fast Kinetics in a Radiation Track<sup>1</sup>  
(N.J.B. Green, M. J. Pilling<sup>2</sup>, S. M. Pimblott, and P. Clifford<sup>3</sup>)

A method is presented for calculating the time-dependent G values and product yields formed in a fast electron track. The calculations are based on an efficient stochastic simulation technique - the Independent Reaction Times (IRT) method - which has previously been developed and validated in detail. The IRT method combines the reactants in pairs and selects reaction times randomly from the appropriate marginal reaction time distributions. Reactions are counted sequentially, starting with the shortest reaction time and limiting subsequent consideration to pairs in the set of remaining particles. The technique is efficient and accurate and is capable of dealing with ionic species, partially diffusion-controlled reactions and reactive products. Our previous calculations based on the IRT method have considered only reactions of small numbers of particles in isolated spurs. A new simulation protocol is presented which efficiently handles the extended distribution and the large number of reactive particles encountered in a radiation track while making use of any isolation that exists on appropriate timescales. The simulated G values at zero time and 0.1  $\mu$ s for a model 22 MeV electron track differ significantly from experimental values and the discrepancy is ascribed to deficiencies in the initial distribution.

---

(1) Submitted for publication in the Journal of Physical Chemistry.

(2) Oxford University, U.K.

(3) Mathematical Institute, Oxford.

---

6. (NDRL-3175) Photochemistry of 3,4,9,10-Perylenetetracarboxylic Dianhydride Dyes. Part 4. Spectroscopic and Redox Properties of Oxidized and Reduced Forms of the Bis(2,5-di-tert-butylphenyl)imide Derivative<sup>1</sup>  
(W.E. Ford<sup>2</sup>, H. Hiratsuka<sup>3</sup>, and P.V. Kamat)

Four oxidation states of the title compound (DBPI) are characterized electrochemically and spectroscopically. The oxidation of DBPI to its radical cation (DBPI<sup>+</sup>•) is irreversible and occurs at an electrode potential of about + 1.1 V vs. SCE. The reductions of DBPI to the radical anion (DBPI<sup>-</sup>•) and DBPI<sup>-</sup> to the dianion (DBPI<sup>2-</sup>) are reversible with reduction potentials of -0.73 V and -0.96 V vs. SCE, respectively. The radical anion is stable with respect to disproportionation. All three electron-transfer products of DBPI, which were produced either by radiolysis or chemical reduction, have intense ( $\epsilon \approx 10^5 \text{ M}^{-1} \text{cm}^{-1}$ ) absorption bands in the visible or near-infrared region, with maxima near 600 nm (DBPI<sup>+</sup>•), 700 nm (DBPI<sup>-</sup>•), or 545 nm (DBPI<sup>2-</sup>). The kinetic parameters of pulse radiolytic oxidation and reduction of DBPI are determined, and the redox potentials of the first excited singlet and triplet states of DBPI are estimated.

---

(1) Submitted for publication in the Journal of Physical Chemistry.  
(2) Bowling Green State University, Bowling Green, Ohio.  
(3) Department of Chemistry, Tokyo Institute of Technology, Ohokayama, Meguro-ku, Tokyo 152, Japan.

---

7. (NDRL-3176) Intermediates in the Charge Transfer and Ligand Labilization Photoreactions of Mo(V)  $\mu$ -oxo -Dimers<sup>1</sup>

(M. Feliz and G. Ferraudi)

The photochemical processes induced in UV-irradiations of  $\text{Mo}_2\text{O}_4(\text{OH}_2)_6^{2+}$  or  $\text{Mo}_2\text{O}_4\text{Cl}_6^{4-}$  respectively have been investigated in a  $\mu\text{s-ns}$  time domain by flash photolysis. In addition to ligand photolabilization, we have observed photoreactions characterized as a reduction of one metal center and oxidation of either coordinated- $\text{H}_2\text{O}$  or coordinated-Cl. Reactions of the primary generated radicals with scavengers and excess Mo(V) complexes were investigated by pulse radiolysis and flash photolysis. The involvement of charge transfer excited states, CTTM, in the photochemistry of the Mo(V) complexes is dis-

cussed.

---

(1) Submitted for publication in Inorganic Chemistry.

---

8. (NDRL-3177) Stochastic Models of Diffusion-Controlled Ionic Reactions in Radiation Induced Spurs. 2. Low Permittivity Solvents<sup>1</sup>  
(N.J.B. Green, M.J. Pilling,<sup>2</sup> S.M. Pimblott and P. Clifford<sup>3</sup>)

The diffusion-controlled recombination of small clusters of ions in low permittivity solvents is considered. A Monte Carlo simulation technique used previously for high permittivity solvents is introduced and discussed briefly. The Independent Reaction Times (IRT) simulation method is described and its implementation for the kinetics of ion clusters is detailed. The IRT approximation is tested against the full Monte Carlo simulation for a variety of random and non-random initial configurations, and against alternative analytic theories. We find the IRT method to be surprisingly accurate under these stringent conditions.

---

(1) Submitted for publication in the Journal of Physical Chemistry.

(2) Physical Chemistry Laboratory, Oxford, U.K.

(3) Mathematical Institute, Oxford, U.K.

---

9. (NDRL-3178) A Laser Flash Photolysis Study of Photodehydroxylation Phenomena of 9-Phenylxanthen-9-ol and Photobehavior of Related Intermediates. Enhanced Electrophilicity of 9-Phenylxanthenium Cation Singlet<sup>1</sup>  
(R.E. Minto<sup>2</sup> and P.K. Das)

In the course of 248 nm laser flash photolysis, solutions of 9-phenylxanthen-9-ol (1) undergo homolytic and heterolytic photodehydroxylation, the relative efficiency of which depends strongly on the solvent nature. Polar/hydroxylic solvents, particularly aqueous mixtures, cause copious formation of 9-phenylxanthenium cation (2), the ground- and excited-state properties of which are conveniently studied by single- and double-laser flash photolysis. In 1:1 H<sub>2</sub>O:MeCN, the quantum yield of carbenium ion generation is 0.8 ± 0.2, only 1% of which evolves through an adiabatic route. Surprisingly, in polar but nonhydroxylic solvents (e.g., acetonitrile and 1,1-dichloro-

ethane) also, the cation is photogenerated at concentrations high enough for time-resolved spectroscopic studies in relatively neutral and inert media. In relatively nonpolar solvents, e.g., n-heptane and benzene, the photolysis of 1 is dominated by homolytic cleavage to 9-phenylxanthenyl radical (3). The short-lived triplets of 1 ( $\tau_T \leq 0.3 \mu s$ ) are also observed in nonaqueous solvents ( $\phi_T = 0.05$  in acetonitrile). In comparison to the weak, fast-decaying, doublet-doublet fluorescence of 3 ( $\lambda_{max}^F = 590 \text{ nm}$ ,  $\tau_T \leq 5 \text{ ns}$ ), the singlet-singlet fluorescence from 2 is intense and long-lived ( $\lambda_{max}^F = 550 \text{ nm}$ ,  $\tau_F = 25 \text{ ns}$  in acetonitrile in the absence of nucleophilic quenchers) and is almost nonquenchable by oxygen ( $k_q \leq 5 \times 10^8 \text{ M}^{-1} \text{s}^{-1}$ ). The electrophilicity of the lowest excited singlet state of 2, measured in terms of rate constants ( $k_q$ ) of bimolecular quenching by anions and lone-pair containing molecules, is considerably more pronounced than that of the ground-state (that is,  $k_q$ 's are higher for the excited state by several orders of magnitude).

---

(1) Submitted for publication in the Journal of the American Chemical Society.  
(2) University of Waterloo, Canada.

---

10. (NDRL-3179) Photophysics of Pyrene-lipid Probes at the Air-water Interface. A Steady State and Time-resolved Study<sup>1</sup>  
(L.K. Patterson and M. Bohorquez)

Several aspects of its excited single state behavior (singlet decay, excimer and exciplex formation, emission spectra) have made pyrene a widely used probe in studies of biochemical structure. Because of its response to changes in microenvironment, pyrene inclusion in natural and artificial molecular assemblies (e.g., monolayers, bilayers, vesicles) can also provide considerable insight into the mechanisms by which molecular organization may alter the kinetics of photochemical processes. With spread monolayers one may change the degree of such organization in a controlled fashion by compression and/or selection of the host lipid matrix, then correlate the ordering of the assembly with photochemical kinetic parameters. Time-resolved and steady-state fluorescence measurements with various pyrene-lipid probes have demonstrated that at the air-water interface, not only assembly organization but also the binding site of the pyrene chromophore on the carrier molecule can play important roles in determining effects of the host lipid matrix on photo-

physical behavior.

---

(1) Submitted for presentation at Regional ACS Meeting, Cleveland, OH, May 30-June 2, 1989.

---

11. (NDRL-3180) Magnetic Field Effects on the Rate of Outer Sphere Electron Transfer Reactions: A Paramagnetic Transition State<sup>1</sup>

(S. Ronco and G. Ferraudi)

The effect of the magnetic field on the rate of outer sphere electron transfer reactions has been investigated as a function of the field intensity, between 0 and 9 Tesla, and at a given temperature. In complexes of  $d^6$  metal ions, i.e. Ru(II) and Co(III), the rate constant exhibits a complex dependence on the field; a complexity associated with field-induced changes of the electronic matrix element and the activation energy. Changes in the activation energy have been investigated as a function of the temperature at a given field intensity. These measurements have shown that the magnetic susceptibility of activation has the large positive values that are expected for a strongly paramagnetic transition state. The magnetic field effects are discussed in terms of symmetry-determined selection rules for the coupling of the initial and final electronic states of the reactions.

---

(1) Submitted for publication in the Journal of Physical Chemistry.

---

12. (NDRL-3181) Colloidal Semiconductors as Photocatalysts for Solar Energy Conversion<sup>1</sup>

(P.V. Kamat and N.M. Dimitrijević)

Considerable attention has been drawn in recent years to develop ultra-fine semiconductor particles which exhibit excellent photocatalytic properties. Size quantization effects, non-linear optical properties and enhanced photoredox properties make quantized colloidal semiconductors potentially useful in the design of photoelectrochemical systems. Photochemical and photophysical processes that directly influence the photocatalytic properties of the semiconductor colloids and the factors that limit the charge transfer at the semiconductor/electrolyte interface are discussed here. Applications

of semiconductor particulate systems in the conversion and storage of solar energy are also described.

---

(1) Submitted for publication in Solar Energy.

---

13. (NDRL-3182) Picosecond Charge Transfer Events in the Photosensitization of Colloidal  $TiO_2$ <sup>1</sup>

(P.V. Kamat)

The charge transfer from the singlet excited anthracene-9-carboxylic acid (9AC) into the conduction band of a large bandgap semiconductor  $TiO_2$  and the recombination of injected charge with the cation radical,  $9AC^{\cdot+}$ , have been time-resolved in the picosecond-nanosecond time domain with the aid of picosecond laser flash photolysis.

---

(1) Submitted for publication in the Journal of the Chemical Society, Chemical Communications.

---

14. (NDRL-3183) Halide Ion Elimination in the Radiolytic Reduction of Polyhalogenated Aromatics<sup>1</sup>

(M. Ye and R.H. Schuler)

Reaction of hydrated electrons with aromatics substituted with both bromine and chlorine results in the production of significant yields of chloride ion and the complementary bromine-substituted phenyl radical. The total yields show that in all cases the reduction is essentially quantitative. For the dihalogenated benzenes and phenols the relative yields of C-Br and C-Cl bond rupture reflect the relative rates of attachment at the Br and Cl positives, indicating that there is no charge transfer on the time scale of the dissociation of the initial anion. In the case of dihalogenated benzoates about 40% of the reduction results in C-Cl bond rupture, suggesting that the added charge initially localized on the carboxyl group is transferred selectively to the chlorine atom. This latter observation indicates that electron affinities of the halogen atoms and possibly solvation effects override carbon-halogen bond energy differences in the radical anions.

---

(1) Submitted for publication in the Journal of Physical Chemistry.

---

15. (NDRL-3184) Stochastic Treatment of Spur Kinetics in Water<sup>1</sup>

(S.M. Pimblott and N.J.B. Green)

The radiolysis of water with low LET electrons produces a spatially nonhomogeneous distribution of highly reactive radicals and ions that is usually described in terms of initially isolated clusters, known as spurs. The recombination of the reactive species is, for the most part, diffusion-controlled and so the kinetics depend upon the encounter times of the reactants.

We have developed an approximate first passage time simulation technique (the Independent Reaction Times method) for modelling spur kinetics. This model relies upon the independent pairs approximation which is implicit in the usual theory of diffusion-controlled rate coefficients.

The Independent Reaction Times model has been used to study the recombination kinetics of clusters of water fragments and to examine the influence of acid and alkali upon the time-dependent behavior and final product yields.

---

(1) Submitted for presentation at Miller Conference on Radiation Chemistry, Windermere, England, April 3-7, 1989.

---

16. (NDRL-3185) The Radiolysis of Cyclohexane with  $^4\text{He}$  Ions<sup>1</sup>

(J.A. LaVerne, G. Foldiak, and R.H. Schuler)

The yields of  $\text{C}_{12}\text{H}_{22}$ ,  $\text{C}_6\text{H}_{10}$ , and  $\text{C}_6\text{H}_{11}\text{I}$  have been measured in the gamma and  $^4\text{He}$  ion radiolysis of cyclohexane with various concentrations of iodine. The yields of  $\text{C}_6\text{H}_{10}$  and  $\text{C}_{12}\text{H}_{22}$  in the radiolysis of neat cyclohexane with  $^4\text{He}$  ions do not change appreciably from 5 MeV (LET = 90 eV/nm) to 20 MeV (LET = 30 eV/nm). In solutions of 1 mM iodine the yield of  $\text{C}_6\text{H}_{11}\text{I}$  decreases with increasing LET while the yields of  $\text{C}_{12}\text{H}_{22}$  and  $\text{C}_6\text{H}_{10}$  increase slightly. This result is consistent with a radical mechanism in which fewer radicals escape the particle track because of greater radical recombination with increasing LET. In the gamma radiolysis the yields of  $\text{C}_{12}\text{H}_{22}$  and  $\text{C}_6\text{H}_{10}$  and  $\text{C}_6\text{H}_{11}\text{I}$  cyclohexane decrease with added  $\text{I}_2$ , suggesting the  $\text{I}_2$  interferes with precursors to the  $\text{C}_6\text{H}_{11}$  radical. Cyclohexyl radical yields are strongly dependent on iodine concentration with 10 MeV  $^4\text{He}$  ions. The decrease in yields of  $\text{C}_6\text{H}_{10}$  and  $\text{C}_{12}\text{H}_{22}$  upon addition of 0.1 mM  $\text{I}_2$  is considerably less with  $^4\text{He}$  ion than with gamma irradiation but at 40 mM  $\text{I}_2$  these yields are very nearly the same for

both radiations.

---

(1) Submitted for presentation at Miller Conference on Radiation Chemistry, Windermere, England, April 3-7, 1989.

---

17. (NDRL-3186) Absolute Kinetics of Dichlorocarbene in Solution<sup>1</sup>  
(J.E. Chateauneuf)

A direct comparison of pulse radiolysis and 266 nm laser flash photolysis (LFP) of liquid carbon tetrachloride reveals identical transient species are observed by nanosecond time-resolved UV-visible absorption spectroscopy.

The reactive intermediate having a characteristic UV absorption band ( $\lambda_{\text{max}} = 330$  nm, band width = 50 nm fwhm) that is observed upon irradiation of  $\text{CCl}_4$  has been kinetically identified as ground-state singlet dichlorocarbene.

Over the years, there have been several assignments of the two major absorption bands observed upon radiolysis of pure  $\text{CCl}_4$ . Initially, the entire UV-visible spectrum observed upon  $\gamma$ -irradiation of polycrystalline  $\text{CCl}_4$  was attributed to  $\text{CCl}_4^+$ . However, liquid phase pulse radiolysis has demonstrated the two bands are independent species and in solution  $\text{CCl}_4^+$  is exceedingly short lived (~ 200 ps). The broad visible absorption band is, in general, believed to be due to  $\text{CCl}_3^+$  as either the free cation or in an associated form.

The UV absorption band has previously been assigned to dichlorocarbene. Isolation of dichlorocyclopropanes in both radiolysis and UV photolysis of  $\text{CCl}_4$  with added olefin strongly suggested dichlorocarbene was produced from highly excited  $\text{CCl}_4$ . The assignment was tentative however, based primarily on the inability to attribute the transient to a cationic or simple free-radical species.

The present study is the first to correlate the UV absorption with the known singlet-carbene chemistry of dichlorocarbene.

---

(1) Submitted for presentation at the 6th Great Lakes Symposium in Photochemistry, Ottawa, Canada, May 12-14.

---

18. (SR-127) Photosensitization of Large Bandgap Semiconductors<sup>1</sup>

(P.V. Kamat)

An attractive technique for the extension of the absorptive range of large bandgap semiconductor involves attachment of organic dyes with high extinction coefficients to the semiconductor surface. Sensitized photoelectrochemical effect at a  $\text{SnO}_2$  electrode has been demonstrated by coating the semiconductor surface with poly(4-vinylpyridine) and incorporating an anionic dye (erythrosin B) into the polymer film. The spectral response and the I-V characteristics of this sensitized photoelectrochemical cell has been obtained by exciting the dye at the electrode surface. The mechanism of the photo-sensitization effect is described.

---

(1) Submitted for publication in Research and Development.

---

Other investigations in progress include:

19. Recombination in Anisotropic Media

(S.M. Pimblott and A. Mozumder)

It is well known that the specific rate for bulk, diffusion-controlled bimolecular recombination is related to the geminate survival probability of a pair. We have shown that this relationship can be used to derive an elegant expression for the homogeneous recombination of neutral reactants in a medium that is anisotropic,  $k = 4\pi\rho\bar{D}$ . This formula is similar to Debye's result for isotropic media  $k = 4\pi RD$ . The spherically symmetric diffusion coefficient  $D$  is replaced by  $\bar{D}$ , the cube root of the determinant of the anisotropic diffusion tensor and the reaction radius  $R$  is superseded by  $\rho$ , a parameter defining the anisotropic reaction surface. The reaction surface defined by  $\rho$  is perpendicular to the principal axes of diffusion as is required by a Smoluchowski model of reaction. When the diffusion tensor is diagonal the reaction surface is an ellipsoid,

$$\frac{\rho^2}{\bar{D}} = \frac{\xi^2}{D_{\xi\xi}} + \frac{\eta^2}{D_{\eta\eta}} + \frac{\zeta^2}{D_{\zeta\zeta}}$$

Treating the motion of the reactants as diffusive, we have derived the time-dependent survival probability and the time-dependent rate coefficient in terms of  $\rho$  and  $\bar{D}$ . This extension is possible because of the boundary condi-

tions that result from using an anisotropic reaction surface perpendicular to the principle axes of diffusion. At present we are examining our theoretical treatment by considering the kinetics of triplet-triplet annihilation in monoclinic crystals of aromatic hydrocarbons where the motion of excitons is anisotropic, e.g. naphthalene or anthracene.

20. Diffusion-controlled Recombination in Multi-pair Clusters

(S.M. Pimblott and N.J.B. Green)

Recently we have developed a stochastic simulation technique for modeling the kinetics of multiple ion-pair clusters in low permittivity solvents. This model, based upon the independent pairs approximation that is implicit in the calculation of time-dependent rate coefficients, accurately reproduces the predictions of a full Monte Carlo simulation of the diffusion and reaction processes. The agreement between Monte Carlo and approximate simulations is somewhat counterintuitive in view of the strong Coulombic forces between ions in low permittivity solvents and suggests that an analytic master equation treatment is possible. We have formulated the recombination kinetics of multi-pair clusters in terms of a general master equation which is applicable to any initial configuration of ions. Solving this set of coupled equations is complicated and the solution is equivalent to that given by our approximate simulation technique. Agreement with Monte Carlo simulation is similarly good. A simplified master equation is obtained when all the cation-anion distances within a cluster are assumed to have the same distribution. This set of equations has been solved and the free-ion yield is a function of the geminate survival probability. The simplified master equation formulation extends the independent pairs approximation to the initial configuration and, consequently, there is a slight underestimate of the free ion yield.

21. Luminescence and Free-Ion Yield due to Heavy Ions in Liquid Argon

(A. Mozumder, A. Hitachi<sup>1</sup> and T. Doke<sup>2</sup>)

The dependence of specific luminescence (light emission per unit absorbed energy) upon the linear energy transfer (LET) of the incident particle in liquid argon has been obtained by collecting data from several laboratories (T. Doke et al., Nuclear Instrumentation and Methods A269, 292, 1988). It reveals a maximum for relativistic heavy ions such as protons to C-ions etc. but a gradual fall on either side of the LET-axis. While the reduction of

light emission for high-energy electrons is easily attributable to escaped charges (thus reducing the formation of excited states), that on the higher-LET side needs a different explanation. For this we propose a quenching mechanism based on a bi-excitonic reaction, i.e.



The probability of this reaction depends on the density of excited states and thus should be of paramount importance in the case of fission fragments. At present we have just finished the calculation of recombination time for  $\alpha$ -tracks in liquid argon. For this the computed recombination time is  $\sim 42$  fs of which  $\sim 1$  fs is required for electron degradation to sub-excitonic energy. About 16 fs is needed to come to the classical turning point in the electrostatic field of the line of positive charges; the residual  $\sim 25$  fs is the time of return to the core. To be consistent the entire recombination time should be much less than the time of exciton self-trapping, estimated to be  $\sim 1$  ps.

We have set up the diffusion-kinetic equation for excitonic motion and combination. A solution, using prescribed diffusion, has been obtained in which the quenching efficiency is a parametric function of the exciton diffusion coefficient, LET, core radius and the specific rate  $k$  of reaction I. Various theoretical and experimental results have been synthesized to evaluate these parameters and reasonable values have been obtained for most of these. The minimum core radius, applicable to  $\alpha$ -tracks in LAR, is  $\sim 4$  Å, increasing to the relativistic limit of  $\sim 40$  Å for  $\sim 1$  GeV/amu Au-ions. The main uncertainty now lies in the rate of reaction I. Writing  $k = \sigma v$  where  $\sigma$  is the reaction cross-section and  $v$ , the excitonic velocity, one knows  $\sigma$  only to an order of magnitude ( $\sim 10$  Å<sup>2</sup>). We shall try to fit  $\sigma$  to the quenching factors obtained experimentally with relativistic ions and then use this result for low velocity ions, e.g., fission fragments.

An experiment for lower energy ( $\sim$  tens of MeV) heavy ions (protons through C-ions) is also being planned using the tandem Van de Graaff generator of the physics department of the University of Notre Dame.

---

(1) Institute of Chemical and Physical Research, Saitama, Japan.

(2) Science and Engineering Research Laboratory, Waseda University, Tokyo, Japan.

---

22. Quantum Mechanical Calculation of the Time Scales of Electron Thermalization and Trapping, and of the Position Distributions in Liquid Water

(S. Pommeret, Y. Gauduel<sup>1</sup> and A. Mozumder)

The principal aim of this study is the computation of the time needed for an ejected electron to get trapped and finally solvated in liquid water and of the associated position distributions. The initial state is simulated as a two-photon ionization of water at 310 nm (8 eV) corresponding to the femto-second experiments of Gauduel et al.<sup>2</sup> Secondarily we wish to investigate such things as the contraction dynamics of the charge distribution during solvation and the influence of ionic strength on the prehydrated electron. The method to be adopted is the numerical solution of the Schrödinger equation by Fast Fourier Transform for a given, simulated configuration of water molecules within a cell. Sufficient information regarding this part of the procedure including the electron-molecule potential<sup>3</sup> is available in one dimension. This has to be extended and the program tested for three dimensions. Models for the simulation of the configuration of the water molecules also need to be developed.

<sup>1</sup> École Polytechnique, ENSTA, Palaiseau, France.

<sup>2</sup> Y. Gaudel et al. "Ultrafast Phenomena V," G. R. Fleming, ed. (1982), Springer Verlag, pp. 308-311.

<sup>3</sup> A. Wallquist et al. J. Phys. Chem. 92, 1721 (1988); J. Schnittker and P. J. Rossky, J. Chem. Phys. 86, 3462 (1987).

23. Fractal Effects on Geminate Processes

(A. Mozumder)

It has been shown by H. Takayusu (J. Phys. Soc. (Japan) 51, 3057, 1982) that fractal effects in diffusive processes involving the selective coordinates of two particles are equivalent to a position-dependent diffusion coefficient. The specific form of the diffusion coefficient may be written as

$$D^{-1}(r) = D_0^{-1} (1 + d/r)$$

where  $r$  is the separation distance,  $D_0$  is the infinite distance diffusion coefficient (or the Brownian value for infinitesimally small mean free path)

and  $d$  is a certain scale length. For neutral diffusion, López-Quintella et al. (Chem. Phys. Lett. 138, 476, 1987) have essentially identified  $d$  with the mean free path of diffusive motion. However its significance for ionic diffusion is not clear, although López-Quintella et al. (J. Chem. Phys. 88, 7478, 1988) have indicated that  $d = a\lambda$  where  $\lambda$  is the mean free path and  $a$  is a constant estimated between 3 and 4 by comparison with certain Monte Carlo computations.

We have set up orthodox diffusion equations for neutrals and ions using this specific form of  $D(r)$  and solved them for geminate escape probability and for the homogeneous (bulk) reaction rate. For ionic geminate pairs the escape probability increases and the specific rate decreases with the mean free path. For neutrals the situation is complicated determined by whether the reaction is mainly diffusion-controlled, or mainly activation-controlled. But in most cases the specific rate decreases with the mean free path. Such effects have been observed by other investigators using the Monte Carlo procedure; however, our method is analytical. It is well-known that decrease of specific rate may result from energetic considerations also (for example, due to relatively small final chemical reaction rate). However, it is not clear how much this effect contributes in a given situation vis-a-vis the effect due to finite mean free path. We are now focussing our attention on this part of the problem.

#### 24. The Radiolysis of Cyclohexane with Helium Ions

(J.A. LaVerne, G. Foldiak, and R.H. Schuler)

The yields of  $C_6H_{10}$ ,  $C_{12}H_{22}$  and  $C_6H_{11}I$  have been measured in the helium ion and gamma radiolysis of cyclohexane with various concentrations of iodine. The yields of  $C_6H_{10}$  and  $C_{12}H_{22}$  are 2.25 and 1.10 molecules/100 eV, respectively, in the radiolysis of neat cyclohexane with 10 MeV helium ions. These yields do not change appreciably from 5 MeV (LET = 90 eV/nm) to 20 MeV (LET = 30 eV/nm). With gamma radiolysis the yields of  $C_6H_{10}$  and  $C_{12}H_{22}$  are found to be 3.12 and 1.76 molecules/100 eV, respectively, which is in very good agreement with the values found in the literature. Addition of 0.1mM of iodine decreases the yields of  $C_6H_{10}$  and  $C_{12}H_{22}$  by 56% and 15%, respectively, with gamma rays but by 86% and 72%, respectively, with 10 MeV helium ions. These results suggest that track processes are much more predominant with helium ions at these times ( $\sim 10 \mu s$ ) than with gamma rays. Product yields are found

to be very sensitive to iodine concentrations with 10 MeV helium ions and at 40 mM of iodine the yields of  $C_6H_{10}$  and  $C_{12}H_{22}$  are found to be 0.61 and 0.30 molecules/100 eV, respectively. Nearly the same yields are found in the gamma radiolysis of 40mM iodine solutions. The yield of  $C_6H_{11}I$  is found to increase with increasing iodine concentration using helium ions because of increased scavenging of the cyclohexyl radical before it recombines. The cyclohexyl iodide yield also increased with decreasing LET because more radicals could diffuse from the track before recombination. With gamma rays it was found that the yield of  $C_6H_{11}I$  did not increase with increasing iodine concentration which suggests that iodine is interfering with processes leading to the production of cyclohexyl radicals. Further work is in progress to determine the yields of cyclohexyl radicals and their mode of formation.

#### 25. Luminescence Due to Ion Recombination in Heavy Ion Tracks

(J.A. LaVerne and B. Brocklehurst)

Ions and excited species have an important role in the radiolysis of hydrocarbons. However, there have been very few studies of these species with heavy particles. The processes by which ions and excited species produce chemically reactive species may be considerably altered because of the high energy deposition density in the track. One method for observing ion combination and charge transfer processes is time-resolved luminescence. Preliminary studies have been made on the helium ion radiolysis of 10 mM PPO in cyclohexane. It is found that at 20 MeV the luminescence consists of fast and slow decay components. The fast decay process is due to geminant recombination which gives a lifetime of a few nanoseconds due to the decay of  $PPO^*$ . The slow component is due to ion recombination and gives a lifetime of about 10 ns. Similar results were found with beta particles. With decreasing ion energy the fast component of the luminescence decreases and at 5 MeV only the slow component of the decay is observed. The increase in track LET from 30 to 90 eV/nm has resulted in processes which prohibit luminescence due to geminant recombination. These processes can be interfering with the initial formation of ion pairs, the transfer of energy to PPO or the quenching of the excited states. Further work with ion and excited state scavengers will help elucidate these very fast processes and their dependence on particle energy deposition density.

26. Resonance Raman Study of p-Phenylenediamine Radical Cation and Its Deprotonated Form

(Q. Sun, G.N.R. Tripathi and R.H. Schuler)

The resonance Raman spectra of p-phenylenediamine radical cation are being examined at several excitation wavelengths, and interesting enhancement patterns have been observed. The prominent bands are observed at  $1645\text{ cm}^{-1}$  ( $\nu_{8a}$  ring stretching),  $1422\text{ cm}^{-1}$  ( $\nu_{7a}$  C-N stretch),  $841\text{ cm}^{-1}$  ( $\nu_1$  ring breathing) and  $1523\text{ cm}^{-1}$  ( $\nu_{8a}$  C-C stretch). Since the  $\nu_{8a}$  is most strongly enhanced in the resonance Raman spectrum, the 480 nm absorption is very likely due to the  $^2B_{1u} \leftarrow ^2B_{3g}$  electronic transition. The assignments of the other electronic transitions are in progress. The resonance Raman spectrum of the neutral  $\text{HNC}_6\text{H}_4\text{NH}_2$  radical has also been recorded. Strongly resonance enhanced are the bands at  $1605\text{ cm}^{-1}$  ( $\nu_{8a}$  ring stretch),  $1493\text{ cm}^{-1}$  ( $\nu_{7a}$  C-N stretch) and  $1383\text{ cm}^{-1}$  ( $\nu_{13}$  C-N stretch) on 480 nm excitation. Two enhanced C-N stretching vibrations indicate non-equivalence of the two C-N bonds. Since the optical absorption spectra of p-phenylenediamine cation radical and its deprotonated neutral radical strongly overlap, the  $pK_a$  of the cation radical can not be determined by the optical absorption technique. The  $pK_a$  value of this radical has been estimated as 13 (0.1 M KOH) by applying the resonance Raman technique.

27. Resonance Raman Study of the Effects of 2,5-Disubstitution on the  $^2A_u \leftarrow ^2B_{3g}$  Electronic Transition of the p-Benzosemiquinone Anion Radical

(Q. Sun, G.N.R. Tripathi and R.H. Schuler)

In a previous study, the 370 nm absorption of the p-benzosemiquinone anion radical ( $\text{Q}^-$ ) was assigned to the  $^2A_u \leftarrow ^2B_{3g}$  transition based on resonance Raman enhancement patterns. This transition in 2,5-dimethyl-, 2,5-dichloro-, and 2,5-dihydroxy-p-benzosemiquinone anion radicals has recently been studied by time-resolved absorption and resonance Raman techniques. In the case of 2,5-dimethyl semiquinone anion radical, the  $^2A_u \leftarrow ^2B_{3g}$  transition shifts to 360 nm. The  $\nu_{7b}$  ( $1115\text{ cm}^{-1}$ ),  $\nu_{8b}$  ( $1430\text{ cm}^{-1}$ ) and  $\nu_1$  ( $707\text{ cm}^{-1}$ ) bands are observed to be strongly resonance enhanced on excitation at 360 nm, but not at 430 nm. The  $^2A_u \leftarrow ^2B_{3g}$  transition shifts to 380 nm in 2,5-dichlorosemiquinone anion radical, and to 440 nm in 2,5-dihydroxysemiquinone radical anion where it is masked by the  $^2B_{1u} \leftarrow ^2B_{3g}$  transition. The

strongly resonance enhanced bands are observed at  $1620\text{ cm}^{-1}$  and  $719\text{ cm}^{-1}$  on  $440\text{ nm}$  excitation and are assigned to the  $\nu_{8a}$  and  $\nu_1$  (ring breathing) modes, respectively.

28. Time-resolved Resonance Raman Studies of Durohydroquinone Cation and the Deprotonated Forms of the Radical

(Q. Sun, G.N.R. Tripathi and R.H. Schuler)

Time-resolved absorption and resonance Raman spectroscopies have been used to examine the radical produced by electron or hydrogen atom transfer to duroquinone. The resonance Raman spectra of durohydroquinone cation, neutral durosemiquinone and durosemiquinone anion radicals are recorded in 30%  $\text{H}_2\text{SO}_4$ , and at  $\text{pH} = 2.5$  and  $\text{pH} = 11.0$  aqueous solutions, respectively. The acid-base equilibrium between the cation radical and neutral radical was observed at 12%  $\text{H}_2\text{SO}_4$  (~ 2.25 M). Strongly resonance enhanced bands were observed at  $1625\text{ cm}^{-1}$ ,  $570\text{ cm}^{-1}$  and  $469\text{ cm}^{-1}$  and assigned respectively to the  $\nu_{8a}$  (ring stretching),  $\nu_{9a}$  (C-CH<sub>3</sub> bending) and  $\nu_{6a}$  (ring deformation) modes for the radical anion, when excitation was at 430 nm. Similar enhancement patterns are observed in the spectra of neutral and cation radical systems.

29. Resonance Raman Study of the Pulse-radiolytic Reactions of Halide Ions in Aqueous Solution

(G.N.R. Tripathi)

Time-resolved resonance Raman spectroscopy is being applied to study the structure and chemistry of transients produced on pulse radiolysis of halide ions in aqueous medium. We find that on pulse irradiation of a 100 mM NaCl solution at neutral pH, Raman signals of Cl<sub>2</sub><sup>·-</sup> radical (excitation at 370 nm) are barely observable. However, when KBr is added to this solution at 1 to 10 mM concentration, Cl<sub>2</sub><sup>·-</sup> signals become prominent. A transient species with Raman bands at 210 and  $390\text{ cm}^{-1}$  is also produced along with the Br<sub>2</sub><sup>·-</sup> radical, at the microsecond time-scale. Studies are in progress to identify this species and to examine its kinetic behavior.

30. Resonance Raman and Fluorescence Studies of Photophysics and Photochemistry of Radical Intermediates

(G.N.R. Tripathi)

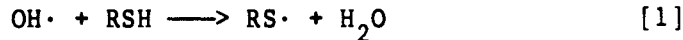
Photophysics of transient radical species produced on pulse radiolysis of

hydroxy-, methoxy-, and amino-benzenes are being examined by time-resolved resonance Raman and fluorescence spectroscopic techniques. Preliminary studies on p-dimethoxybenzene and hydroquinone systems appear to indicate that while photoionization is the primary event on photolysis of their H adducts, the OH adducts mostly undergo photodissociation. The fluorescence emission from the neutral p-benzosemiquinone, and its resonance Raman spectra provide a means for studying the acid-base equilibria in the excited as well as the ground electronic states of the radical. These studies are currently in progress.

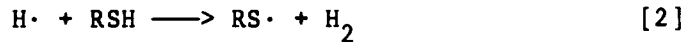
31. The pH Dependence of the RS<sup>•</sup>/RS<sup>•</sup>SR<sup>-</sup> Equilibrium

(S. Mezyk)

The further investigation of the sulfhydryl RS<sup>•</sup>/RS<sup>•</sup>SR<sup>-</sup> equilibrium constant dependence on pH has shown that similar behavior to that observed previously for penicillamine (Q-126) occurs also for cysteine and cysteamine. However, inconsistencies and scatter in the reported yields and rate constant for the oxidation reactions



and



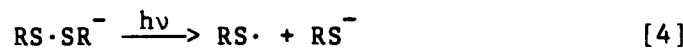
for all three RSH compounds give large uncertainty in the measured data.

The accurate measurement of these values is difficult, as the RS<sup>•</sup> species have low extinction coefficients ( $\epsilon \sim 400 \text{ M}^{-1} \text{ cm}^{-1}$ ) and the rate constant for the forward equilibrium reaction



is of similar magnitude ( $k \sim 10^{10} \text{ M}^{-1} \text{ s}^{-1}$ ) to reactions [1] and [2].

However, using a combined LINAC/laser experiment, the dimer anion species can be created according to the above reactions, and then homolytically cleaved by a single laser pulse to again give the sulfhydryl radical,



whose recombination rate constant (reaction [3]) can then be independently measured. From simple kinetics, the concentration and pH dependence of this process allows accurate determination of the equilibrium constants, and the rate constants for reactions [1] and [2].

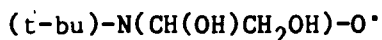
### 32. An ESR/HPLC Study on MNP Spin Trapping in Methanolic Solutions

(K.J. Liu and K.P. Madden)

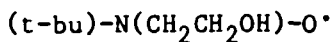
Study on the spin trapping with 2-methyl-2-nitrosopropane (MNP) has shown that MNP reacts with radicals to form relatively stable spin adducts not only in its monomeric form, but also in the form of dimer. These spin adducts normally have a lifetime of a few hours to a couple of days, and will either react with each other or rearrange to achieve a more stable structure. To isolate and identify the products of spin adduct transformation, we are using HPLC to isolate and resolve the various components of solution after spin trapping, and ESR to identify the radical components isolated.

Steady-state ESR shows two radicals in solutions with maximum dimer and minimum monomer concentrations of MNP. They are identified as the hydroxymethyl radical and the nitroxide radical  $(t\text{-bu})\text{N}(\text{CH}_2\text{OH})\text{O}^\bullet$ , with ESR parameters  $a(\text{N, NO}) = 15.51$  Gauss,  $a(\text{H, CH}_2) = 6.20$  Gauss,  $a(\text{H, OH}) = 0.27$  Gauss. Although the nitroxide radical is a spin adduct, its lifetime is only a few seconds, as the radical either rearranges or reacts with other species to form a more stable structure.

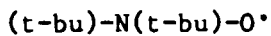
Analysis of the aqueous MNP-methanol solution subsequent to Co(60) gamma irradiation shows three major radiolysis products, two of which are nitroxide radicals. These radicals are normally stable for one or two days, and therefore may be detected and studied at leisure. The two radicals collected from HPLC separation come from the reactions of hydroxymethyl radical with dimeric and monomeric MNP, respectively. In the solution rich in dimeric MNP, the ESR spectrum is tentatively assigned to the radical A,



with the parameters  $a(\text{N, NO}) = 15.78$  Gauss,  $a(\text{H, CH}) = 1.57$  Gauss,  $a(\text{H, CH}_2) = 0.97$  Gauss. This adduct is stable at ambient temperature for one day, and will rearrange to become radical B,



and radical C, di-t-butyl nitroxide,



The ESR spectrum parameters for B are  $a(\text{N, NO}) = 16.17$  Gauss,  $a(\text{H, CH}_2) = 11.02$  Gauss,  $a(\text{H, CH}_2) = 0.51$  Gauss. The assignment is supported by the evidence from mass spectroscopy. In the mass spectrum of the radicals, the existence of A and B are indicated by large peaks at mass-to-charge ratios of 148 and 132, respectively.

### 33. Microwave Absorption Measurements at a Second Microwave Frequency

(D.B. Toublanc and R.W. Fessenden)

An apparatus has been constructed to carry out microwave absorption and dispersion measurements on photochemical transients at around 3 GHz. Previous measurements were at 9.1 GHz. Measurements at a single frequency provide only limited information on the rotational motion (relaxation time) of the transient species because the ratio of dispersion to absorption uniquely defines a relaxation time only if further details of the relaxation behavior is known (single relaxation time or a distribution of times). Data at a second frequency help greatly in further defining the behavior. The new apparatus which uses a resonator consisting of a 1/4 wavelength transmission line shorted on one end has comparable sensitivity to that found at 9 GHz with the standard apparatus. Measurements on the excited states of Michler's ketone and fluorenone, on diphenylcyclopropenone and on the charge carriers in semiconductor powders all show a higher ratio of dispersion to absorption than the values found at 9 GHz. This behavior is as expected and strengthens the interpretation given to those data. Further experiments with the excited state of 9,9'-bianthryl and the exciplexes of dimethylaniline with anthracene and pyrene will be carried out to refine measurement of their dipole moments.

### 34. Reactivity of Cu-Alkyl Complexes

(E. Baumgartner and G. Ferraudi)

Time-resolved spectroscopy in the picosecond time domain has shown that a  $\text{Cu}^{\text{II}}(\text{aq})$ -alkyl intermediate is produced with  $t_{1/2} < 10$  ps in flash irradiation.

tions of  $\text{Cu}^{\text{II}}(\text{aq})$ -polyacrylic acid complexes. The formation of the alkyl complexes in the flash photolysis of  $\text{Cu}^{\text{II}}(\text{TIM})$ -polyacrylic acid is slower than in the aqueous complexes; only a fraction of the photogenerated  $\text{Cu}^{\text{I}}(\text{TIM})^+$  is converted to the alkyl product. In the microsecond time domain, we have observed the decay of the Cu(I) complex with second-order kinetics whose rate depends on the molecular weight of the polyacrylic acid. This effect, attributed to the local concentrations of the transient Cu complexes, is currently being investigated by flash photolysis of several Cu(II) complexes bound to various polyelectrolytes.

35. Magnetic Field Effects on the Reactivity of Coordination Complexes

(S. Ronco and G. Ferraudi)

Previous studies from this laboratory have shown that intense magnetic fields change the rates of the coordination complexes' ground and excited state reactions. In  $\text{CrL}_3^{3+}$  (L = polypyridine ligand) we have observed magnetic field-induced changes in the emission spectra and in the emission rate. These specific magnetic field perturbations of the ligand field excited states are presently being investigated with a series of  $\text{Cr}(\text{macrocycle})\text{X}_2^+$  complexes where strong spin-orbit coupling controls the relaxation rates. The emission from charge transfer states in Re complexes, e.g.,  $\text{Re}(\text{CO})_3(\text{benzoylpyridine})_2\text{Cl}$ , has been investigated at zero field and room temperature. The effect of the field on the emission spectrum and on the rate of emission is currently being investigated as a function of the field intensity and temperature.

36. The Photochemical Reactivity of the Clusters  $\text{Mo}_6\text{Cl}_8\text{Y}_6^{2-}$

(B. Kraut and G. Ferraudi)

$(\text{Bu}_4\text{N})_2\text{Mo}_6\text{Cl}_8\text{Y}_6$ -type compounds (where Y = F, Cl, Br, I, SCN or oxygen-donor organic ligand) have been prepared in order to investigate the role of the outer ligands in the photochemistry of this cluster group. Substitution of the outer  $\text{Cl}^-$  ligands by halide or pseudo-halide ions generally causes red shifts while substitution by organic ligands causes blue shifts in the UV-visible absorption spectra. Although the emission spectra are independent of the Y ligand, the substitution of  $\text{Cl}^-$  by  $\text{Y}^-$  reduces the rather long emission lifetime with respect to the 180  $\mu\text{s}$  lifetime of the  ${}^*\text{Mo}_6\text{Cl}_{14}^{2-}$  in acetonitrile. The largest radiationless relaxation rate has been detected in the case of the  $\text{Mo}_6\text{Cl}_8(\text{CH}_3\text{COO})_6^{2-}$ , where the emission lifetime is only 60 ns. In

laser flash photolysis experiments we observed a common transient absorption peak at 400 nm having the same lifetime as the emission, that can be assigned as the excited state. The other parts of the transient spectra, however, change ligand by ligand.

The mixed order kinetics of these optical changes and the sensitivity to experimental conditions indicate that different photochemical processes - such as excited state-excited state reactions, photosubstitution and photoredox reactions - are taking place simultaneously.

The behavior of these complexes on biphotonic excitation is under investigation.

### 37. Pulse Radiolytic Studies of the Redox Reactions of Metal Macrocyclic Complexes Bounded to Polyelectrolytes

(S. Ronco)

Some tetraazamacrocyclic complexes of Ni are catalysts in the reduction of  $\text{CO}_2$  in aqueous solutions. The stability of these metal macrocycles complexes (when they are in unusual oxidation states) can be affected by the electrostatic field of a polyelectrolyte. The studies described below will establish the mechanism of the  $\text{CO}_2$  reduction when the Ni species are subject to interactions with a polyelectrolyte.

Divalent nickel complexes of  $\text{Me}_6[14]\text{-4,11-dieneN}_4$  or  $\text{Me}_6[14]\text{-aneN}_4$  were respectively reduced with  $e^-_{\text{aq}}$  in  $10^{-4}$  M aqueous solutions containing PAH (PAH = polyacrylic acids) at  $\text{pH} = 6.5$ . In these experiments the concentration of the acrylic group in the solution was always  $10^{-3}$  M. The monovalent complexes generated by reduction of the parent Ni(II) macrocycles exhibited lifetimes which were dependent on the molecular weight of the PAH used. The disappearance of the Ni(I) species was accelerated by factors of  $3 \times 10^3$  and  $2 \times 10^3$  (relative to solutions without PAH) with polyacrylic acids of molecular weight  $2.5 \times 10^5$  and  $2 \times 10^6$ , respectively, but was retarded by a factor of ten when the molecular weight was  $2 \times 10^3$ .

A similar effect was observed for the  $\text{Cu}(\text{TIM})^{2+}$  (TIM =  $\text{Me}_4[14]\text{-1,3,8,10-tetraeneN}_4$ ) complex in the same conditions as above. In this case, the reaction was 80 and 10 times faster with PAH of molecular weight  $2 \times 10^6$  and  $2 \times 10^3$ , respectively. The dependence of the decay lifetime of the monovalent species on the molecular weight of the polyacrylic acid is in agreement with some flash photolysis observations.

The decay of the monovalent complex of Ni was also followed in solutions containing polyvinylsulfonic acid (MW = 2,000) and in solutions containing polyvinylsulfonic acid saturated with CO<sub>2</sub>. Both the formation and disappearance of the Ni(I) species were slower when working with polyvinylsulfonic acid than in solutions containing only the Ni complex. The transient complexes formed in the reduction of CO<sub>2</sub> are being studied by pulse radiolysis. The trapping of the intermediates and the effect of other polyelectrolytes on the reaction mechanism is being considered for future experiments.

38. Photophysical and Photochemical Studies of Metal-polypyridine Complexes  
(R. Berger)

The photophysics and electrochemical behavior of mononuclear as well as both heteronuclear and homonuclear bimetallic polypyridine complexes are currently under investigation.

The complex  $[(bpy)_2Ru(dpp)Ru(bpy)_2](PF_6)_4$  (bpy = 2,2'-bipyridine; dpp = 2,3-dipyridopyrazine) has been prepared. This complex is of interest since, unlike most polypyridine bridged binuclear Ru(II) systems, it is emissive in room temperature fluid solution. In ethanol, this complex has an emission maximum of 800 nm ( $\phi = 9.0 \times 10^{-4}$ ) and an excited state lifetime of 80 ns.

The excited state absorption spectrum of the complex consists of maxima at 375 and 460 nm with bleaches at 325, 430 and 540 nm. Correcting for ground state depletion, maxima occur at 340, 460 and 610 nm.

Cyclic voltammetry of the complex (~0.8 mM in N,N'-dimethylformamide/0.1 M tetrabutylammonium hexafluorophosphate on a platinum disk) reveals reversible reductions at -0.61, -1.05, -1.41, -1.64 and -1.80 V vs. Ag/AgCl. These reduction waves correspond to sequential reduction of the five ligands, starting with the bridging ligand. In addition, two oxidation waves are observed at 1.47 and 1.66 V vs. Ag/AgCl. These waves correspond to the sequential oxidation of the two Ru(II) centers.

An absorption spectrum of the complex recorded at -0.9 V vs. Ag/AgCl where the complex is singly-reduced reveals the presence of maxima at 340 and 480 nm and a shoulder at 615 nm. Subtracting the spectrum of the unreduced complex results in a difference spectrum virtually identical in shape to the difference ESA spectrum, excepting the 5-20 nm shifts. In the electrochemical case there is considerably less bleaching in the visible region. In the excited state, one of the Ru centers is oxidized, decreasing the residual charge transfer to

the unreduced ligands by a factor of 2 relative to the electrochemically reduced state where two Ru(II) centers remain.

Future work will involve reductive spectroelectrochemistry of the mono-nuclear analogue as well as oxidative spectroelectrochemistry of the binuclear complex. The latter case will involve the observation of a mixed-valence binuclear Ru system.

39. Picosecond Time-resolved Studies on Biphenylene

(A. Samanta, C. Devadoss and R.W. Fessenden)

It has long been proposed that rapid non-radiative transition in biphenylene results from a change of geometry in the first excited singlet state. Although this idea has been widely accepted among photophysicists, there is no direct experimental evidence in favor of this proposal. We have performed picosecond time-resolved absorption studies to look directly into the process of geometry change. In the course of our studies we have found that excitation of a cyclohexane solution of biphenylene at 355 nm leads to two distinct absorption bands in the range 400-760 nm; a broad and weak band at 650 nm and strong band at 430 nm. The two bands exhibit different decay behavior and therefore, they arise from two different excited states of biphenylene. Based on the similarity of the lifetime of the 650 nm band (~250 ps) with that obtained from fluorescence decay measurement we assign this band to the transition from the lowest emitting singlet state of biphenylene. The short wavelength band with a lifetime of only ~ 8 ps is also found to arise from the  $S_1$  state of biphenylene. Two different lifetimes of the  $S_1$  state can be explained only if the 8 ps component represents the Franck-Condon state while the 250 ps component arises from the relaxed  $S_1$  state which has a different geometry. These results, therefore, represent the first direct experimental demonstration of the geometry change that occurs in the lowest excited singlet state of biphenylene.

40. Picosecond and Nanosecond Studies of the Photoreduction of Benzophenone by Amines

(C. Devadoss and R.W. Fessenden)

In continuation of our study of the photoreduction of benzophenone (BP) by amines, we have observed the absorption spectrum of the elusive Dabco<sup>+</sup>, which has a broad band from 400-550 nm with  $\lambda_{\text{max}}$  at 480 nm. By introducing trace

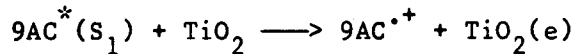
amounts of  $O_2$  over the solution and selectively quenching the benzophenone anion we are able to observe the  $Dabco^{+}$  alone. The quenching by oxygen is effective in acetonitrile but not in benzene which means either that the nature of the ion pair is different in these two solvents or that the quenching mechanism which may involve CT is prohibited in nonpolar benzene.

The photoreduction of BP by diethylaniline (DEA) has been carried out in benzene, methanol, *t*-BuOH and acetonitrile. In contrast to the case of  $Dabco$ , quenching by DEA does not produce  $BP^{+}$  in benzene, but the characteristic bands due to  $BP^{+}$  and  $DEA^{+}$  ( $\lambda_{max} = 470$  nm) have been observed in methanol and acetonitrile. In methanol, the decay rate of  $BP^{+}$  is much faster than  $DEA^{+}$  and in MeOD the decay of  $BP^{+}$  is slowed down. This isotopic effect indicates that  $BP^{+}$  may abstract  $H^{+}$  from the alcohols and also the counter ion  $DEA^{+}$  may influence the reactions of the ion pair. No absorption signals of  $BP^{+}$  and  $DEA^{+}$  have been observed in *t*-BuOH in nanosecond experiments but the picosecond experiments clearly indicate that both radical ions are formed. They decay to products within 10 ns.

#### 41. Photoelectrochemistry in Semiconductor Particulate Systems

(P.V. Kamat)

Subnanosecond photochemical events on colloidal  $TiO_2$  surfaces which control the charge injection from electronically excited anthracene-9-carboxylic acid ( $9AC^*$ ) into the conduction band of the semiconductor are being studied with picosecond laser flash photolysis. Laser pulse excitation (355 nm) of  $9AC$  in colloidal  $TiO_2$  produced the cation radical of the sensitizer ( $9AC^{+}$ ) which was characterized from its absorption maximum at 720 nm.



The formation of  $9AC^{+}$  was prompt and was completed within the laser pulse duration. The transient absorption spectra recorded at various excitation intensities showed that the intensity dependence of  $9AC^{+}$  yield was linear at laser intensities below 1 mJ. The back reaction between the injected charge and the cation radical followed first-order kinetics with a rate constant of  $1 \times 10^{10} s^{-1}$ . Such a rapid recombination is a major limiting factor in controlling the sensitization efficiency. Efforts are being made to employ sacrificial donors in this system, which could quickly react with the cation radical and regenerate the sensitizer at the semiconductor surface.

42. Photophysics and Photochemistry of Small Metal Chalcogenides in Polymer Films

(K.R. Gopidas and P.V. Kamat)

Ultrafine semiconductor particles of CdS and CdSe have been prepared in a polymer environment by exposing Cd<sup>2+</sup> substituted Nafion polymer to H<sub>2</sub>S atmosphere. The particle size of the semiconductor was controlled by varying the Cd<sup>2+</sup> concentration in the film and the time of H<sub>2</sub>S exposure. These semiconductor particles exhibited strong emission in the visible region (400-650 nm). The emission decay was multiexponential with lifetimes ranging from 700 ps - 1  $\mu$ s. The short lifetime component which contributed to the decay of emission near the absorption edge is attributed to the recombination of electrons from the conduction band. Trapped charge carriers were found to dominate the emission at longer wavelengths. The emission spectrum is being time-resolved with laser flash photolysis to elucidate the photophysical processes of the quantized semiconductor particles. The effects of polymer environment on the charge transfer processes of CdS and CdSe particles will also be studied.